MANSOURA JOURNAL OF BIOLOGY
Official Journal of Faculty of Science, Mansoura University, Egypt
E-mail: scimag@mans.edu.eg ISSN: 2974-492X

Optimization of iron oxide nanoparticles biosynthesis: a selection of the efficient bactericidal and/or bacteriostatic type against pathogenic bacteria

Sara Abd-Elghany[1,*], Hosam Salaheldin[2], Hoda kabary[3], Ashraf Elsayed[1]

[1] *Department of Botany, Faculty of Sciences, University of Mansoura, Egypt,*

[2] *Division of biophysics, Department of physics, faculty of science, University of Mansoura, Egypt,*

[3] *Department of agricultural microbiology, national research center, Egypt.*

**** Corresponding author** e.mail: saraabdelghany572@gmail.com; Tel. +201024361891*

Received:6/8/2023
Accepted: 27/8/2023

Abstract The recent widespread infectious diseases associated with pathogenic bacteria, i.e., *Staphylococcus aureus*, *Salmonella typhi*, *Escherichia coli* and *Klebsiella pneumonia* are a serious health issue. Regarding the potentiality of magnetotactic bacteria, *Pseudomonas aeruginosa kb1* (KT962901) in biosynthesis of nanoparticles, this research study was designed to improve the synthesis conditions of iron oxide nanoparticles (IONPs) and subsequently evaluate the efficacy of each factor in controlling the growth of specific pathogenic bacteria. In the research methodology, the different factors were investigated to optimize the biosynthesis process, i.e., medium type, aeration conditions, concentration, salt type and point of salt addition. The shape and structure of the synthesized IONPs were confirmed using Fourier transform infrared (FTIR) spectroscopy, Scanning Electron Microscopy (SEM), Energy Dispersive X-ray diffraction (EDX) analysis, Zeta potential and Dynamic light scattering (DLS). The well diffusion method was used to assess the efficiency of IONPs in suppressing the growth of target bacteria. The study's findings showed that clear zones against two or three of the tested bacteria were present in 13 of the 36 tested samples utilized in the initial screening to treat the pathogenic bacteria. There are just two samples (trials no. 6 and 13) that have demonstrated outstanding antibacterial action against both Gram-negative and Gram-positive bacteria after the second screening using higher concentrations of the 13 patches. In conclusion, optimizing the process of iron oxide nanoparticles biosynthesis by *Pseudomonas aeruginosa* kb1 may provide a more effective method in controlling some pathogenic bacteria.

keywords: nano-iron, antibacterial activity, magnetotactic bacteria, biosynthesis

Introduction

It was believed that bacterial diseases could be readily controlled after Alexander Fleming discovered penicillin in 1928 and subsequent scientific advancement over the 20th century **[1]**. But since the 1950s, doctors have had to deal with emerging and reemerging infectious diseases, which have created serious problems for the public's health and the economy.

The advancement of better treatment and survival was made possible by the medical microbiology discoveries made towards the end of the 19th century, which demonstrated how bacteria were the root cause of several of the major diseases of the period. Not surprisingly, some people believed that bacteria were responsible for all diseases at this point, giving rise to the theory that bacterial infections may cause cancer **[2]**.

Early 1990s investigations that determined *Helicobacter pylori* to be the cause of stomach cancer led to a paradigm shift in the relationship between microbiological organisms and malignancies. **[3]**. *H. pylori* was the first bacterium species to be recognized by the World Health Organization as a certain factor in the development of human cancer in 1994. *Salmonella typhi* and gallbladder cancer, *E. coli* and colorectal cancer, *Staphylococcus aureus*, and *Klebsiella* spp. and bladder cancer are some of the additional species linked to cancer.

It is commonly known that a rod-like Gram-negative bacterium called *Salmonella typhi* belongs to the family of Enterobacteriaceae causes enteric fever or typhoid. These bacteria build up in the gallbladder and cause a chronic infection without any symptoms **[4]**. According to epidemiological research conducted in *S. typhi*-endemic areas, Gall cholelithiasis, which poses a considerable danger of gallbladder cancer, occurred in the majority of chronically infected carriers. *S. typhi* produces typhoid toxins that have the potential to cause cancer by damaging the DNA and altering the infected cells' cell cycle **[5]**.

Staphylococcus aureus is a significant human pathogen that can cause a variety of infections, recently rose to the top of the list of drug-resistant organisms, particularly in crowded areas and hospital with poor sanitation **[6]**. Due to its rising occurrence, it evolved many strains that were resistant to various antibiotic classes, including methicillin, which called (*MRSA*). To defend itself from the human immune system, the *MRSA* pathogen exhibits several behaviors. It secretes substances that evade the innate human immune system by inhibiting neutrophil and phagocytosis activity. furthermore, avoiding the complement system, which protects humans against invasions that cause genotoxicity and DNA damage **[7].**

the development of bacterial and cancer cells resistance pathways to commonly used medications is a significant factor in the ineffectiveness of these agents in treating disease although attempts have been increased to circumvent this problem **[8, 9]**. Richard Feynman, a well-known physicist, initially proposed the idea of nanotechnology in 1959. Norio Taniguchi then used the word "nanotechnology" in 1974. Recently, in 1986, the book of Eric Drexler's "The Engine of Creation; The Beginning of the Era of Nanotechnology" introduced the notion of nanotechnology in the sector of molecular technology **[10]**. The application of nanoparticles (NPs) with dimensions of 1-100 nm in diverse sectors of fundamental and industrial sciences is the most basic definition of nanotechnology. It also refers to the production of materials at the atomic, molecular, and supermolecular levels. **[11]**. Due to their high surface-to-volume ratio and enhanced optical activities compared to their mass state, NPs are employed in a range of industries, including health, food, aerospace, and agriculture **[12]**.

Researchers, scientists, and technologists are now aware of the value of nanotechnology in biology, medicine, and industry **[13]**. Additionally, NPs are employed in antibacterial vaccinations to prevent bacterial infections, bacterial detection systems for microbial diagnostics, and antibiotic delivery systems for use during treatment **[14]**. A significant benefit of using NPs to limit bacterial growth in diverse diseases is the specificity of the methods by which they affect bacterial metabolic activities **[14-16]**. According to the investigations, several NPs exhibit strong antibacterial activities against a range of pathogens, including genotoxic bacteria **[17-21]**. Numerous elements affect how NPs affect bacteria, including their shape, preparation process, kind of stabiliser, and other characteristics **[14, 19, 22, 23]**.

Recent decades have seen a tremendous expansion in nanotechnology, particularly with the creation of better methods for the production of NPs **[24]**. There are a number of "bottom-up" and "top-down" methodologies that can be used to synthesize NPs employing gaseous, solid, and liquid precursors **[25]**. The bottom-up approach creates NPs from atoms and molecules by chemical or self-aggregation reactions in contrast to the top-down technique, which begins by breaking up the bulk material into tiny bits using mechanical, chemical, or a mix of both methods [26]. Controlling particle size, shape, size distribution, composition, and degree of aggregation is necessary to choose the best option **[26]**.

Researchers recently became aware that organisms and biological materials may produce nanoparticles (NPs) from their salt precursors and stabilize them in solution using more environmentally friendly methods that do not require the use of expensive and hazardous chemicals **[27, 28]**. the industrial revolution, excessive urbanization, and an expanding population have negatively impacted the Earth's atmosphere by introducing toxic compounds to

the environment **[25]** Therefore, the green synthesis approach for NPs provides an attractive alternative to the conventional chemical and physical synthesis methods **[29, 30]**. Where metal NPs and metal oxide NPs may be produced using plants, bacteria, fungi, algae, yeasts, and lichens **[31]**. Due to the utilization of metal precursors to produce metal NPs and metal oxide NPs, this procedure is classified as a bottom-up approach **[32]**.

NPs can be classified as either metallic or non-metallic; the metallic nanoparticles seem to hold the most promise. They have a variety of behaviors against various pathogens **[33-35]**. Silver nanoparticles (Ag NPs) and gold nanoparticles (Au NPs) are the most extensively researched metal nanoparticles. Metal oxide nanoparticles with demonstrated antibacterial properties involve magnesium oxide (MgO NPs), iron oxide (Fe_2O_3 NPs), copper oxide (CuO NPs), zinc oxide (ZnO NPs), and titanium oxide nanoparticles (TiO_2 NPs) **[36]**. Additionally, nanoparticles can be mixed with antibiotics and other nanomaterials to enhance their antibacterial properties.

Iron oxide nanoparticles (IONPs) stand out among the other types of nanoparticles due to their biocompatibility, accessibility, and their established effectiveness for a variety of applications including the production of sensors, drug delivery, cancer therapy, and biomedical treatments **[37]**. IONPs have advantageous qualities like enhanced membrane characteristics, a large surface area, a high tensile strength, and tiny particle sizes. Hematite (-Fe_2O_3), maghemite (-Fe_2O_3), goethite (FeOH), and magnetite (Fe_3O_4) are some of the distinct phases of iron oxide crystallites. One of the most typical, organic, and environmentally friendly materials is hematite **[38]**.

2. Materials and methods

2.1. Culturing magnetotactic bacteria (MTB)

The magnetotactic bacteria, *Pseudomonas aeruginosa* kb1 (KT962901) was previously identified **[39]**, which was obtained from microbial culture collection of the Agricultural Microbiology Department, National Research Centre, Cairo, Egypt. *P. aeruginosa* kb1 cells were grown in two different media, nutrient broth medium which contains (g/L): 5 peptone, 5 NaCl and 3 beef extract **[40]** and M3 medium which contains (g/L): 0.1 $MgSO_4.7H_2O$, 0.15 KH_2PO_4, 0.40 NH_4Cl, 0.1 yeast extract, 2.38 Hepes, 3.0 sodium pyruvate, 3.0 peptone, and 1mL from EDTA trace element solution according to Widdel and Bak **[41]**. Both media were prepared for culturing *P. aeruginosa* kb1 under different growth conditions.

The following experiments were implemented to determine the optimum growth conditions for synthesis of iron NPs with the most potent antibacterial activity against some common pathogens *E. coli*, *K. pneumonia*, and *S. aureus* which were obtained from the Bacteriology Lab, Botany Department, Faculty of Science, Mansoura University, Mansoura, Egypt. Both degree of aeration (aerobic or anaerobic) and type of added iron salt (Four different salt preparations; ferrous sulphate, ferric sulphate, and a mixture of ferric and ferrous sulphate (1:1), as well as ferric chloride salt). were adjusted either during the bacterial growth or/and after collecting the supernatant for the synthesis process. The resulting pellets were screened for antibacterial activity and the most potent was selected for propagation and further sophisticated analysis.

The pH was adjusted to 6.8 after establishing the prior condition, and the autoclave was run at 121°C for 30 minutes. Then all the treatments (35 samples) were inoculated with 1ml *P. aeruginosa* kb1 inoculum (OD_{600} of 0.8), incubated at 30 °C, 3 days in a static incubator for anaerobic conditions and at 150 rpm for aerobic conditions. After that, the cultures of bacteria were centrifuged (6,000 rpm for 20 min.) to collect the supernatant for the processes of IONPs biosynthesis and pellets were applied for magnetosome extraction after ultra-sonication.

2.2. Extraction of intracellular magnetosomes

Following three distilled water rinses, the pellets were placed in 100 ml of a buffer solution that contained 20 mM Hepes and 4 mM EDTA. Ultrasonication was employed as part of a physical method to harvest magnetosomes and disperse cells. Before being crushed with an ultrasonicator (600 W/cm^2, 2.5 min, and 30 pluses) in an ice bath, the bacterial cells were immersed in PBS buffer and exposed

to three cycles of freezing and thawing **[42]**. A powerful permanent magnet was used to gather the released magnetosomes from the bacterial cells extracted. Through numerous PBS buffer washes, the cell debris and other contaminants were eliminated **[39]**.

2.3. Extracellular biosynthesis of iron nanoparticles

Aqueous solutions of 1 mM $FeSO_4.7H_2O$, $Fe_2(SO_4)_3.5H_2O$, $FeCl_3.6H_2O$ (50 mL) and a mixture of ferric and ferrous sulphate (1:1) were prepared. 50 µL from each solution was added to 50 ml supernatant in a 100 ml Erlenmeyer flask after adjusting pH at 7.5. The whole mixture was incubated at 37 ºC, 200 rpm for 2 days. After the incubation period, the mixture was centrifuged (10,000 rpm for 10 minutes). The pellets were washed three times using deionized water and oven dried at 80 ºC for 20 hr.

2.4. Assessment of antibacterial activity

The antibacterial activity of the 35 produced iron nanoparticles and the extracted magnetosomes was done by the well diffusion method **[43]**. The nutrient agar plates were prepared, and three pure cultures of *E. coli*, *K. pneumonia*, and *S. aureus*, were inoculated using the spread plate method. Then, using a sterile borer, the wells with a diameter of 6 mm were created in the agar plates. 50 µL of the prepared IONPs (50 mg/mL) were injected into the wells. The plates were then kept in the incubator for 24 hours at 37 °C.

Out of 36 treatments, 13 were chosen to investigate their antimicrobial impact in a second screening trial based on the results of antimicrobial testing using the agar diffusion technique against *E. coli*, *S. aureus*, and *K. pneumonia* with two higher concentrations of iron sources 2.5mM (125µL), and 5mM (250 µL) iron source in 50 ml supernatant solution under the same conditions against the three strains used before in addition to two new strains *S. typhi* and *MRSA*. According to the second antimicrobial test results, two best treatments (13 and 6) were selected for scaling up to be used in further analysis.

2.5. Large-scale biosynthesis of IONPs under conditions of trial no. 13 and 6

For scaling up the production of IONPs (trial no. 13 and 6) 3 L. nutrient broth medium was prepared with ferrous sulfate inoculated by *P. aeruginosa* kb1 and incubated for 3 days in aerobic conditions, at 30 ºC temperature and 150 rpm shaking conditions. the biosynthesized IONPs were oven dried and stored for the next characterization and applications.

2.6. Characterization of biosynthesized IONPs

Fourier transform infrared (FTIR) transmittance was evaluated in the 400-4000 cm^{-1} range using Burker Vertex 80 (Germany). Also, in order to examine the structural and textural characteristics of the synthesized iron oxide nanoparticles, dynamic light scattering (DLS), zeta potential and scanning electron microscopy-energy dispersive spectroscopy (SEM-EDS) were used. EDS analysis was carried out using a scanning electron microscopy Joel microscope equipped with 40 kV and equipped with an EDS detector.

3. Results and Discussion

3.1. Microorganism and Cultural Conditions

This bacterium which was previously identified as *Pseudomonas aeruginosa* kb1**[39]** was preserved and cultured on nutrient agar (NA) medium overnight at 30°C **(Figure 1)**

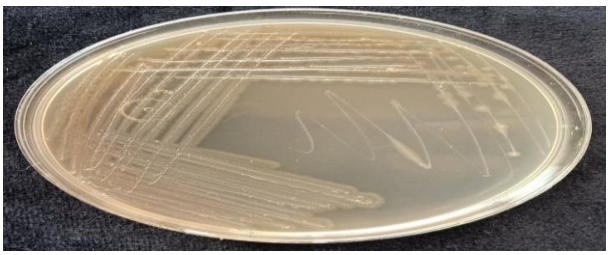

Figure 1: *P. aeruginosa kb1* growth on NA medium.

3.2. Biosynthesis of iron NPs by magnetotactic *P. aeruginosa kb1* bacterial strain

Thirty-five different types of IONPs in addition to the extracted magnetosomes were synthesized by *P. aeruginosa kb1* using different conditions **(Table 1)**. From the quantity measurements of IONPs, trial number 1 recorded the maximum yield production as a value of 55 mg whereas trial number 21 and 31 produced the lowest yield as a value of 1 mg. Generally nutrient broth medium was better than both types of M3 media in the biosynthesis of IONPs. It was obvious that the addition of

iron salts in the nutrient broth medium and supernatant produced a high amount of iron NPs.

Whereas the addition of these salts to the other M3 media produced variable amounts of iron NPs. Iron sulfate compounds produced IONPs in quantity more than chloride compounds. Regarding the aeration condition, the anaerobic condition was better than aerobic in the production of IONPs in all types of used media. *P. aeruginosa* kb1 being a magnetotactic bacteria, they are all microaerophiles or anaerobes which prefer little to no oxygen because nitrates or other oxidized forms of nitrogen (NO_2, NO) serve as electron acceptors in a series of reductions that results in molecular nitrogen, allowing them to grow in the absence of oxygen **[44]**. The specific technique by which bacteria can produce IONPs is not entirely established. According to studies, nanoparticles are often created by a reduction process, where metal ions are initially trapped on the surface or within the microbial cells. Enzymes are then used to reduce the trapped metal ions to nanoparticles **[45]**.

Nitrate reductases, which are frequently present in transmembrane form and are discharged into the environment in lower amounts, are involved in the anaerobic respiration of *P. aeruginosa* **[46]**. These molecules serve as an electron source for NADPH-dependent nitrate reductases during the substrate reduction process. These enzymes may reduce metal ions to release them as elemental cores, which are the building blocks of nanoparticles, in addition to employing nitrate salts as a substrate **[47, 48]**. A similar mechanism was shown to be in play in Bacillus cereus, where the bacterial-produced nitrate reductase was revealed to be used in iron reduction into nanoparticles **[49]**.

Table 1. Variable conditions used for the production of iron oxide NPs**.**

No.	Media	Adding Fe Salt	Aeration	Salt Type	NPs Wt.(mg)
1	Nutrient Broth	Medium + Supernatant	Anaerobic	Ferric Sulfate	55.0
2				Ferrous Sulfate	15.4
3				Mix	5.0
4				Ferric Chloride	13.7
5			Aerobic	Ferric Sulfate	20.0
6				Ferrous Sulfate	15.8
7				Mix	26.6
8				Ferric Chloride	15.8
9		Supernatant	Anaerobic	Ferric Sulfate	7.2
10				Ferrous Sulfate	9.5
11				Mix	5.0
12				Ferric Chloride	6.1
13			Aerobic	Ferric Sulfate	5.9
14				Ferrous Sulfate	6.4
15				Mix	5.2
16				Ferric Chloride	4.0
17	M3 Medium Without Ferric Citrate	Medium + Supernatant	Anaerobic	Ferric Sulfate	13.8
18				Ferrous Sulfate	8.1
19				Mix	8.4
20				Ferric Chloride	5.1
21			Aerobic	Ferric Sulfate	10.0
22				Ferrous Sulfate	1.0
23				Mix	2.1
24				Ferric Chloride	1.7
25		Supernatant	Anaerobic	Ferric Sulfate	14.5
26				Ferrous Sulfate	4.0
27				Mix	20.0
28				Ferric Chloride	11.8
29			Aerobic	Ferric Sulfate	7.6
30				Ferrous Sulfate	15.6
31				Mix	12.8
32				Ferric Chloride	1.0
33	M3 Medium With Ferric Citrate	Supernatant	Anaerobic	Ferric Sulfate	20.0
34				Ferrous Sulfate	20.0
35				Ferric Chloride	20.0
36		Free from additional salt		Magnetosomes	10.0

3.3. First screening: antibacterial activity of biosynthesized IONPs against three pathogenic bacteria

From the 36 patches of IONPs applied for treating the Gram-negative Bacteria *E. coli* and *K. pneumonia* and Gram-Positive *S. aureus*, 5 patches of the synthesized IONPs showed clear zones against the three types of the tested bacteria (trial no. 1, 5, 13, 22, and 23). 8 patches exposed clear zones against two types of bacteria (trial no. 2, 3, 4, 6, 8, 14, 24, and 31) whereas 15 patches showed inhibition against only one type (trial no. 7, 9, 10, 11, 12, 17, 18, 19, 20, 21, 27, 29, 32, 34 and 35) on the other hand 8 patches revealed no activity against any bacterial type (trial no. 15, 16, 25, 26, 28, 30, 33 and 36) **(Table 2).** The 13 exposed patches were tested in higher concentrations against two new bacteria in addition to the three previously tested pathogens in order to conduct a second screening of antibacterial activity.

Table 2. First qualitative screening of antibacterial activity using different patches of IONPs against E. coli, Klebsiella pneumonia, Staphylococcus aureus.

No.	Inhibition zone		
	E. coli	K. pneumonia	S. aureus
1	+ ve	+ ve	+ ve
2	+ ve	- ve	+ ve
3	+ ve	- ve	+ ve
4	+ ve	- ve	+ ve
5	+ ve	+ ve	+ ve
6	+ ve	- ve	+ ve
7	- ve	+ ve	- ve
8	+ ve	+ ve	- ve
9	+ ve	- ve	- ve
10	+ ve	- ve	- ve
11	- ve	+ ve	- ve
12	+ ve	- ve	- ve
13	+ ve	+ ve	+ ve
14	- ve	+ ve	+ ve
15	-ve	-ve	-ve
16	- ve	- ve	- ve
17	- ve	+ ve	- ve
18	- ve	+ ve	- ve
19	- ve	+ ve	- ve
20	+ ve	- ve	- ve
21	+ ve	- ve	- ve
22	+ ve	+ ve	+ ve
23	+ ve	+ ve	+ ve
24	- ve	+ ve	+ ve
25	- ve	- ve	- ve
26	- ve	- ve	- ve
27	+ ve	- ve	- ve
28	- ve	- ve	- ve
29	-ve	+ ve	- ve
30	- ve	- ve	- ve
31	+ ve	- ve	+ ve
32	- ve	+ ve	- ve
33	- ve	- ve	- ve
34	- ve	+ ve	- ve
35	- ve	+ ve	- ve
36	- ve	- ve	- ve

+ve: observable clear zone, -ve: no clear zone.

E. coli and *K. pneumonia* had been inhibited by 17 patches of IONPs trials while 19 trials had no activity against both of them whereas only 13 patches of IONPs had

activity against *S. aureus* while it was resistant to 23 trials **(Figure2)**.

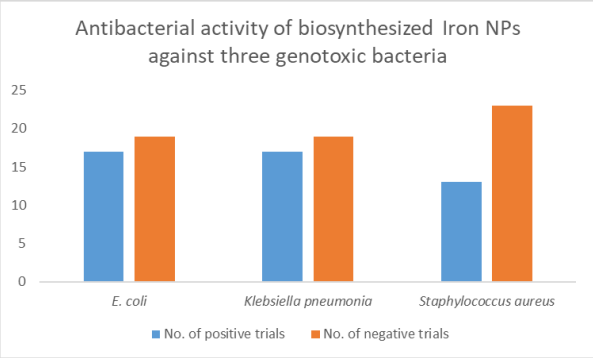

Figure. 2. Antibacterial activity using different patches of IONPs against *E. coli*, *K. pneumonia*, and *S. aureus*.

3.4. Second screening: antibacterial activity of biosynthesized IONPs against five pathogenic bacteria

After the synthesis of IONPs using higher concentrations of iron salts added to the media or supernatant, 13 treatments were applied against five bacteria *E. coli*, *K. pneumonia*, *S. aureus*, *S. typhi* and *MRSA* bacterial strains **(Table 3 and Figure 3)**. Results from the 13 treatments showed that 4 treatments (trial no.13, 6, 21 and 30) inhibited the growth of two or more types of bacteria whereas 9 treatments of IONPs had no activity against all tested bacterial strains. All the four IONPs that showed positive results were synthesized under aerobic conditions from *P. aeruginosa* kb1, two treatments (13 and 6) were prepared by culturing in a nutrient broth medium and the other two treatments (21 and 30) were cultured in an M3 medium. The two treatments based on a nutrient broth medium showed higher antibacterial activity, so they were selected for scaling up for further analysis.

E. coli, K. pneumonia, S. aureus, S. typhi, and MRSA all showed inhibitory zones of 14 mm, 15 mm, 15 mm, and 17 mm, respectively, in the treatment 13. While Treatment 6 demonstrated no activity against *MRSA*, it had inhibitory zones of 7 mm with *E. coli*, 5 mm with *K. pneumonia*, 7 mm with *S. aureus*, and 12 mm with *S. typhi*. Additionally, treatment 21 demonstrated no action against *MRSA* and had inhibition zones of 2 mm for *E. coli*, 7 mm for *K. pneumonia*, 4 mm for *S. aureus*, and 2 mm for *S. typhi*. Furthermore, treatment 30 had no activity against the other examined bacterial strains but had a 4 mm inhibition zone with *S. typhi* and 2 mm with *S. aureus*. Finally, the most significant inhibition zone measured from treatment using trial number 13 against *S. typhi* was 17 mm, while the minimum inhibition zone measured from treatment using trial number 13 against *MRSA* was 2 mm.

The oxidative stress caused by reactive oxygen species (ROS) including superoxide radicals (O_2-), hydroxyl radicals (-OH), hydrogen peroxide (H_2O_2), and singlet oxygen (O_2), which could destroy bacterial proteins and DNA, may be the root cause of the antibacterial action demonstrated by IONPs **[50, 51]**.

Gram-positive bacteria *S. aureus* and *MRSA* are found to be less sensitive to IONPs than Gram-negative bacteria *E. coli, K. pneumonia* and *S.typhi* due to the presence of a thicker layer of peptidoglycan **[52]**. The presence of an outer membrane with a thick coating of peptidoglycan serves as a permeability barrier which can also be permeable to the antibacterial effect of nanoparticles**[53]**.

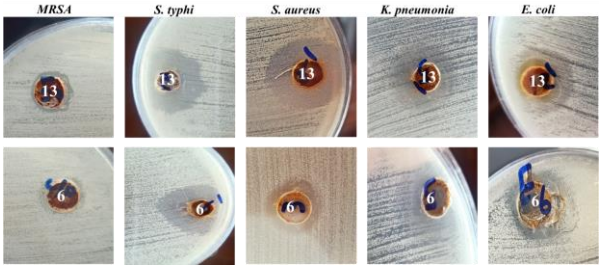

Figure. 3. Representative plates showing positive results of antibacterial activity (inhibition zone) using different treatments of IONPs against different pathogenic bacteria. The numbers 13 and 6 indicate the trial's number.

3.5. Large-scale biosynthesis of IONPs under conditions of trial no. 6 and 13

When the aqueous iron salt solution was applied to bacterial supernatant during the large-scale biosynthesis of IONPs under the conditions of trials no. 6 and 13, the color changed to a dark brownish color after 48 hours which is the first optical indication of the success of the synthesis process **(Figure 4)**. The conditions of trial no. 13 were better than the conditions of trial no. 6 in scaling up

the biosynthesis of IONPs, where it produced a higher quantity (2 g) over the low quantity (1 g) from trial no. 6 After scaling up. A similar type of colour shift in $FeSO_4$ salt solution during the production of IONPs has been seen in recent papers utilizing plant extract. **[54, 55]**.

Table 3. Second quantitative screening of antibacterial activity using different treatments of IONPs against pathogenic bacteria.

No.	Media	Adding Fe Salt	Aeration	Salt Type	Inhibition Zone (mm)				
					E. coli	*K.p*	*S.a*	*S.t*	*MRSA*
1	Nutrient Broth	Medium+ Supernatant	Anaerobic	Ferric Sulfate	-ve	-ve	-ve	-ve	- ve
2				Ferrous Sulfate	- ve	- ve	- ve	- ve	- ve
3				Mix	- ve	- ve	- ve	- ve	- ve
4				Ferric Chloride	- ve	- ve	- ve	- ve	- ve
5			Aerobic	Ferric Sulfate	- ve	- ve	- ve	- ve	- ve
6				Ferrous Sulfate	7	5	7	12	- ve
8				Ferric Chloride	- ve	- ve	- ve	- ve	- ve
13		Supernatant	Aerobic	Ferric Sulfate	14	15	15	17	2
14				Ferrous Sulfate	-ve	-ve	-ve	-ve	-ve
21	M3 Medium Without Ferric Citrate	Medium + Supernatant	Aerobic	Ferrous Sulfate	2	7	4	2	- ve
22				Mix	- ve	- ve	- ve	- ve	- ve
23				Ferric Chloride	- ve	- ve	- ve	- ve	- ve
30		Supernatant		Mix	- ve	- ve	2	4	- ve

+ve: observable clear zone, -ve: no clear zone, *K.p*: *K. pneumonia*, *S.a*: *S. aureus*, *S.t*: *S. typhi*

Figure. 4. Dark brown color of IONPs from trial no. 6 after the biosynthesis using *P. aeruginosa* kb1.

3.6. Characterization of the two synthesized IONPs

3.6.1. FTIR Analysis

One of the analytical methods used for detecting the functional groups and proteins that participate in the biosynthesis process is FTIR. Under infrared radiation in the 400–4000 cm^{-1} range, the FTIR analysis of the bacterial extract and the biosynthesized IONPs spectra were compared. **Figure 5a, b and c** reveals that the two samples (13 and 6) had the three characteristic peaks for the Fe-O bond at 558 cm^{-1}, 670 cm^{-1}, and 866 cm^{-1} **(Figure 5b)** and 551 cm^{-1}, 637 cm^{-1}, and 850 cm^{-1} **(Figure 5c)**, respectively. These results are consistent with those of **Basavegowda, Mishra [56]**. This might be explained by the fact that the bands between 400 and 650 cm^{-1} are connected to the Fe-O bonds in a number of different modes, such as stretching and vibration modes **[57]**. The Fe-O bonding of magnetite nanoparticles is indicated by the bands at 425 cm^{-1} and 557 cm^{-1}. While the metal-oxygen band at 425 cm^{-1} was attributed to the octahedral-metal stretching of Fe-O, the metal-oxygen band at 557 cm^{-1} was related to intrinsic stretching vibrations of metal at the tetrahedral site. The hydroxyl group of a water molecule or iron hydroxides found in the samples are responsible for the bands about 1650 cm^{-1} and 3400–3425 cm^{-1}. According to the aforementioned results, the supernatant's various functional groups, such as polyphenols, ketones, and organic acids, were responsible for reducing Fe^{2+} and Fe^{3+}.

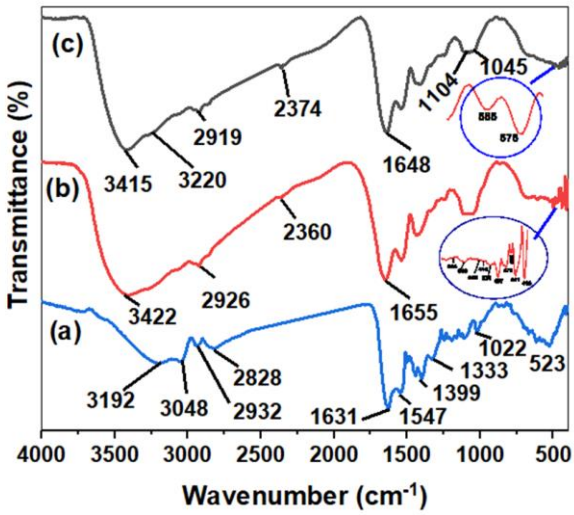

Figure 5. FTIR spectrum of the green synthesized IONPs using magnetotactic bacteria (a) Bacteria extract, (b) Fe_3O_4 NPs, and (c) Fe_2O_3 NPs.

3.6.2. Scanning Electron Microscopy with Electron Diffraction Spectroscopy

The morphology, dimensions, and form of the IONPs were revealed using SEM assessments. The synthesis of Fe_3O4 (Magnetite) may have been carried out based on the shape of the synthesised IONPs from Trial No. 13 as shown in **Figure 6a**. Since then, due to its better magnetic characteristics, electrical conductivity, and biocompatibility, Fe_3O_4 (Magnetite) has received more attention than other iron oxides or ferrite spinel oxides. While **Figure 6b** showed that trial number 6 synthesized IONPs were almost of the hematite (-Fe_2O_3) and/or maghemite (-Fe_2O_3) type. The EDS examination proved the samples of synthesized IONPs were pure. The main peaks of the IONPS from trial number 13 EDS spectrum are shown in **Figure 6c** for Fe and O; Fe weight-based content was 10.32 percent, while O weight-based content was 33.22 percent. Because the samples weren't properly washed, there were a few minor impurities of N and S. Typically, when iron oxide NPs are made from ferric sulphate, sulphur is seen. whereas the significant peaks of IONPS from trial no. 6 are seen in the EDS spectra in **Figure 6d** for Fe, O, and C. the Fe weight-based content was (33.34 %), the O weight-based was (49.73 %), while the C weight-based was (33.92). In addition to these, there were two minor contaminants in the sample: N and P from the media components that were present on the surface of the NPs. But the O at 0.4 keV was linked to the IONPs production of Fe oxides **[58, 59]**. Similar outcomes, demonstrating the existence of Fe and O peaks in the EDX analysis, were found in the prior publication **[60]**.

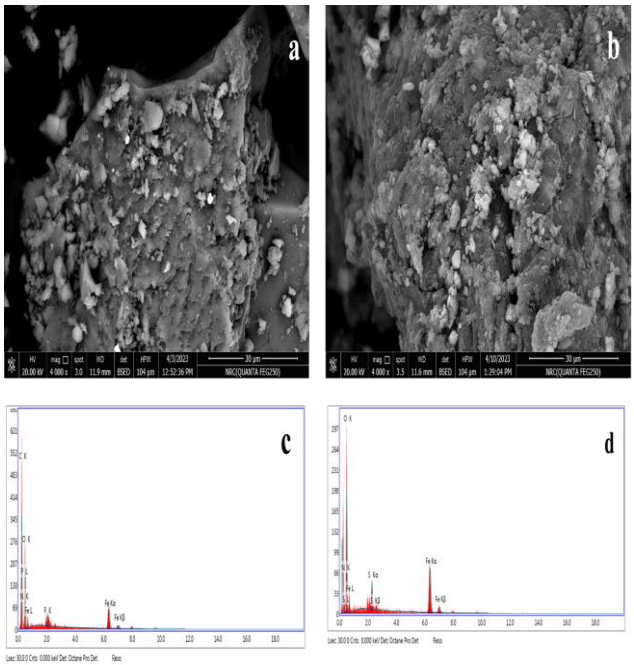

Figure 6. (a–b) SEM image showing morphology; (c) EDX data of green synthesized Fe_3O_4 NPs from trial no. 13 (d) EDX data of green synthesized Fe_2O_3 NPs from trial no. 6.

3.6.3. Dynamic light scattering and Zeta potential

The hydrodynamic size and *PDI* value of Fe_3O_4 NPs from trial no. 13 were measured as 1111 nm and 0.176, respectively **Figure 7a**. While, for the other sample Fe_2O_3 NPs the hydrodynamic average size and *PDI* were 1127 nm and 0.538, respectively **Figure 7b**. Furthermore, Zeta potential measurements were used to assess the stability of the nanoparticles. The capacity of the particles to repel one another electrostatically is reflected by the measurement of net charge on the surface of the nanoparticles. where the colloidal suspension is more stable as the value increased. However, as for the synthesized Fe_3O_4 and Fe_2O_3 samples the zeta potential was measured at -9.56 and +9.96, respectively as shown in **Figure 7c-d**. The stability of the particles was proved to be an excellent as the zeta potential existed in the 30 mv range **[61]**. Therefore, the synthesized either Fe_2O_3 or Fe_3O_4 NPs with a little or good stability. The negative zeta

potential data of Fe_3O_4 revealed that the created NPs are stable and have a constant level of stability throughout thirty days **[62]**.

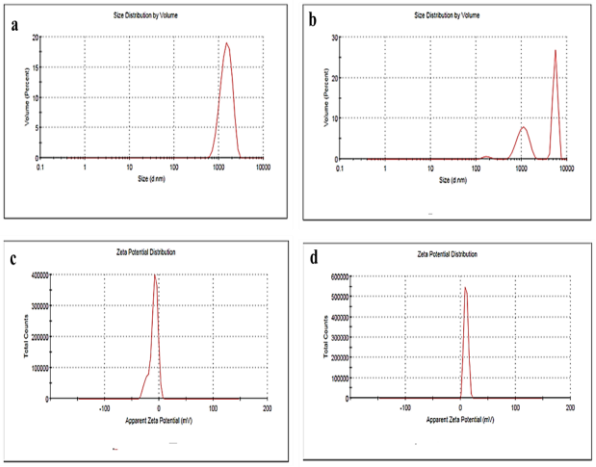

Figure 7. Particle size distribution and Zeta potential of the synthesized IONPs using magnetotactic bacteria. a; particle size distribution of Fe_3O_4. b; particle size distribution of Fe_2O_3. c; Zeta potential of Fe_3O_4. d; Zeta potential of Fe_2O_3

Conclusions

Pseudomonas aeruginosa kb1 (KT962901) served as the reducing and stabilizing agents in the process for the synthesis of iron NPs. Gram-positive and Gram-negative bacteria are both effectively combatted by iron NPs outstanding antibacterial properties. Consequently, this approach would be a low-cost, straightforward, and environmentally friendly way to create iron NPs, which might be applied in for water treatment.

References

.1 Lewis, K. (2013). Platforms for antibiotic discovery, Nature Reviews Drug Discovery **12(5)**: 371-387.

.2 Lax, A.J. and Thomas, W.J.T.i.m. (2002). How bacteria could cause cancer: One step at a time, **10(6)**: 293-299.

.3 Kim, S.S.;Ruiz, V.E.;Carroll, J.D. and Moss, S.F.J.C.l. (2011). Helicobacter pylori in the pathogenesis of gastric cancer and gastric lymphoma, **305(2)**: 228-238.

.4 Di Domenico, E.G.;Cavallo, I.;Pontone, M.;Toma, L. and Ensoli, F.J.I.j.o.m.s. (2017). Biofilm producing salmonella typhi: Chronic colonization and development of gallbladder cancer, **18(9)**: 1887.

.5 Koshiol, J.;Wozniak, A.;Cook, P.;Adaniel, C.;Acevedo, J.;Azócar, L.;Hsing, A.W.;Roa, J.C.;Pasetti, M.F. and Miquel, J.F.J.C.M. (2016). Salmonella enterica serovar typhi and gallbladder cancer: A case–control study and meta-analysis, **5(11)**: 3310-3235.

.6 Cuervo, S.I.;Cortés, J.A.;Sánchez, R.;Rodríguez, J.Y.;Silva, E.;Tibavizco, D. and Arroyo, P.J.E.i.y.m.c. (2010). Risk factors for mortality caused by staphylococcus aureus bacteremia in cancer patients, **28(6)**: 349-354.

.7 McGuinness, W.A.;Kobayashi, S.D. and DeLeo, F.R.J.P. (2016). Evasion of neutrophil killing by staphylococcus aureus, **5(1)**: 32.

.8 Andrei, L.;Kasas, S.;Garrido, I.O.;Stanković, T.;Korsnes, M.S.;Vaclavikova, R.;Assaraf, Y.G. and Pešić, M.J.D.R.U. (2020). Advanced technological tools to study multidrug resistance in cancer, 48: 100658.

.9 Jordt, H.;Stalder, T.;Kosterlitz, O.;Ponciano, J.;Top, E. and Kerr, B. (2020). Coevolution of host–plasmid pairs facilitates the emergence of novel multidrug resistance. Nat ecol evol **4**: 863–869.

.10 Chen, S. and Liang, X.-J.J.S.C.L.S. (2018). Nanobiotechnology and nanomedicine: Small change brings big difference, Springer. **61**: 371-372.

.11 Madkour, L.H.;Madkour, L.H.J.N.M.F. and Applications. (2019). Introduction to nanotechnology (nt) and nanomaterials (nms): 1-47.

.12 Cao, H.-L.;Liu, C.;Cai, F.-Y.;Qiao, X.-X.;Dichiara, A.B.;Tian, C. and Jian, L.J.W.R. (2020). In situ immobilization of ultra-fine ag nps onto magnetic ag@ rf@ fe3o4 core-satellite nanocomposites for the rapid catalytic reduction of nitrophenols, 179: 115882.

.13 Alavi, M. and Webster, T.J.J.N. (2020). Nano liposomal and cubosomal formulations with platinum-based anticancer agents: Therapeutic advances and challenges, **15(24)**: 2399-2410.

.14 Wang, L.;Hu, C. and Shao, L.J.I.j.o.n. (2017). The antimicrobial activity of nanoparticles: Present situation and

prospects for the future: 1227-1249.
.15 Raghunath, A. and Perumal, E.J.I.j.o.a.a. (2017). Metal oxide nanoparticles as antimicrobial agents: A promise for the future, **49(2)**: 137-152.
.16 Ficai, D.;Oprea, O.;Ficai, A. and Maria Holban, A.J.C.P. (2014). Metal oxide nanoparticles: Potential uses in biomedical applications, **11(2)**: 139-149.
.17 Singh, R.;Smitha, M.;Singh, S.P.J.J.o.n. and nanotechnology. (2014). The role of nanotechnology in combating multi-drug resistant bacteria, **14(7)**: 4745-4756.
.18 Singh, R.;Nawale, L.U.;Arkile, M.;Shedbalkar, U.U.;Wadhwani, S.A.;Sarkar, D. and Chopade, B.A.J.I.j.o.a.a. (2015). Chemical and biological metal nanoparticles as antimycobacterial agents: A comparative study, **46(2)**: 183-188.
.19 Assa, F.;Jafarizadeh-Malmiri, H.;Ajamein, H.;Anarjan, N.;Vaghari, H.;Sayyar, Z. and Berenjian, A.J.N.R. (2016). A biotechnological perspective on the application of iron oxide nanoparticles, **9:** 2203-2225.
.20 Gupta, A.;Saleh, N.M.;Das, R.;Landis, R.F.;Bigdeli, A.;Motamedchaboki, K.;Campos, A.R.;Pomeroy, K.;Mahmoudi, M. and Rotello, V.M.J.N.F. (2017). Synergistic antimicrobial therapy using nanoparticles and antibiotics for the treatment of multidrug-resistant bacterial infection, **1(1)**: 015004.
.21 Gabrielyan, L.;Hakobyan, L.;Hovhannisyan, A. and Trchounian, A.J.J.o.a.m. (2019). Effects of iron oxide (fe3o4) nanoparticles on escherichia coli antibiotic-resistant strains, **126(4)**: 1108-1116.
.22 Lee, C.;Kim, J.Y.;Lee, W.I.;Nelson, K.L.;Yoon, J.;Sedlak, D.L.J.E.s. and technology. (2008). Bactericidal effect of zero-valent iron nanoparticles on escherichia coli, **42(13)**: 4927-4933.
.23 Chatterjee, S.;Bandyopadhyay, A. and Sarkar, K.J.J.o.N. (2011). Effect of iron oxide and gold nanoparticles on bacterial growth leading towards biological application, **9**: 1-7.
.24 Leso, V.;Fontana, L. and Iavicoli, I.J.N.T. (2019). Biomedical nanotechnology: Occupational views, **24**: 10-14.
.25 Taran, A.;Zahid, A.;Mironiuc, M.J.T.J.o.E. and Business. (2017). Foreign ownership and financial disclosure in central and eastern europe, **10(2)**: 151-168.
.26 Loza, K.;Epple, M.;Maskos, M.J.B.R.t.N.P.M.;Aspects, C. and Approaches, M. (2019). Stability of nanoparticle dispersions and particle agglomeration: 85-100.
.27 Oza, G.;Reyes-Calderón, A.;Mewada, A.;Arriaga, L.G.;Cabrera, G.B.;Luna, D.E.;Iqbal, H.M.;Sharon, M. and Sharma, A.J.J.o.M.S. (2020). Plant-based metal and metal alloy nanoparticle synthesis: A comprehensive mechanistic approach, **55**: 1309-1330.
.28 Monga, Y.;Kumar, P.;Sharma, R.K.;Filip, J.;Varma, R.S.;Zbořil, R. and Gawande, M.B.J.C. (2020). Sustainable synthesis of nanoscale zerovalent iron particles for environmental remediation, **13(13)**: 3288-3305.
.29 Bartolucci, C.;Antonacci, A.;Arduini, F.;Moscone, D.;Fraceto, L.;Campos, E.;Attaallah, R.;Amine, A.;Zanardi, C. and Cubillana-Aguilera, L.M.J.T.T.i.A.C. (2020). Green nanomaterials fostering agrifood sustainability, 125: 115840.
.30 Hebbalalu, D.;Lalley, J.;Nadagouda, M.N.;Varma, R.S.J.A.S.C. and Engineering. (2013). Greener techniques for the synthesis of silver nanoparticles using plant extracts, enzymes, bacteria, biodegradable polymers, and microwaves, **1(7):** 703-712.
.31 Rao, T.N.;Babji, P.;Ahmad, N.;Khan, R.A.;Hassan, I.;Shahzad, S.A. and Husain, F.M.J.S.J.o.B.S. (2019). Green synthesis and structural classification of acacia nilotica mediated-silver doped titanium oxide (ag/tio2) spherical nanoparticles: Assessment of its antimicrobial and anticancer activity, **26(7)**: 1385-1391.
.32 Pourakbar, L.;Siavash Moghaddam, S.;Popović-Djordjević, (2020) J.J.S.A.R.N.f.P.G. and Development.. Synthesis of metal/metal oxide nanoparticles by green methods and their applications: 63-81.

.33 Mba, I.E.;Nweze, E.I.J.W.J.o.M. and Biotechnology. (2020). The use of nanoparticles as alternative therapeutic agents against candida infections: An up-to-date overview and future perspectives, **36:** 1-20.
.34 Rasheed, T.;Bilal, M.;Li, C. and Iqbal, H.J.C.p.b. (2017). Biomedical potentialities of taraxacum officinale-based nanoparticles biosynthesized using methanolic leaf extract, **18(14)**: 1116-1123.
.35 Liao, Z.;Zhang, W.;Qiao, Z.;Luo, J.;Erpuding, A.;Niwaer, A.;Meng, X.;Wang, H.;Li, X.;Zuo, F.J.J.o.c. and science, i. (2020). Dopamine-assisted one-pot synthesis of gold nanoworms and their application as photothermal agents, **562:** 81-90.
.36 Möhler, J.S.;Sim, W.;Blaskovich, M.A.;Cooper, M.A. and Ziora, Z.M.J.B.a. (2018). Silver bullets: A new lustre on an old antimicrobial agent, 36(5): 1391-1411.
.37 Tanaka, S.;Kaneti, Y.V.;Septiani, N.L.W.;Dou, S.X.;Bando, Y.;Hossain, M.S.A.;Kim, J. and Yamauchi, Y.J.S.M. (2019). A review on iron oxide-based nanoarchitectures for biomedical, energy storage, and environmental applications, **3(5)**: 1800512.
.38 Nizamuddin, S.;Siddiqui, M.;Mubarak, N.;Baloch, H.A.;Abdullah, E.;Mazari, S.A.;Griffin, G.;Srinivasan, M. and Tanksale, A.J.N.m.i.w.p. (2019). Iron oxide nanomaterials for the removal of heavy metals and dyes from wastewater: 447-472.
.39 Kabary, H.;Eida, M.F.;Attia, M.M.;Awad, N.;Easa, S.M.J.A.R. and Biology, R.i. (2017). Magnetotactic characterization and environmental application p. Aeruginosa kb1 isolate: 1-10.
.40 Kawsar, S.M.;Nishat, S.;Manchur, M.A. and Ozeki, Y.J.I.L.C.P.A. (2016). Benzenesulfonylation of methyl α-d-glucopyranoside: Synthesis, characterization and antibacterial screening, **64**: 95-105.
.41 Widdel, F. and Bak, F.J.T.p.a.h.o.t.b.o.b.e., (1992) isolation, identification, applications.. Gram-negative mesophilic sulfate-reducing bacteria: 3352-3378.
.42 Xie, J.;Liu, X.;Liu, W. and Qiu, G.J.P.i.M.B. (2005). Extraction of magnetosome from acidthiobacillus ferrooxidans: 7-10.
.43 Al-Yousef, H.M.;Amina, M.;Alqahtani, A.S؛.Alqahtani, M.S.;Malik, A.;Hatshan, M.R.;Siddiqui, M.R.H.;Khan, M.;Shaik, M.R. and Ola, M.S.J.P. (2020). Pollen bee aqueous extract-based synthesis of silver nanoparticles and evaluation of their anti-cancer and anti-bacterial activities, **8(5)**: 524.
.44 Crespo, A.;Pedraz, L.;Astola, J. and Torrents, E.J.F.i.m. (2016). Pseudomonas aeruginosa exhibits deficient biofilm formation in the absence of class ii and iii ribonucleotide reductases due to hindered anaerobic growth, 7: 688.
.45 Singh, O.V. (2015). Bio-nanoparticles: Biosynthesis and sustainable biotechnological implications, John Wiley & Sons.
.46 Hulkoti, N.I.;Taranath, T.J.C. and Biointerfaces, s.B. (2014). Biosynthesis of nanoparticles using microbes—a review, **121**: 474-483.
.47 Mols, M.;De Been ،M.;Zwietering, M.H.;Moezelaar, R. and Abee, T.J.E.m. (2007). Metabolic capacity of bacillus cereus strains atcc 14579 and atcc 10987 interlinked with comparative genomics, **9(12)**: 2933-2944.
.48 Nath, D.;Banerjee, P.J.E.t. and pharmacology. (2013). Green nanotechnology–a new hope for medical biology, **36(3)**: 997-1014.
.49 Fatemi, M.;Mollania, N.;Momeni-Moghaddam, M. and Sadeghifar, F.J.J.o.b. (2018). Extracellular biosynthesis of magnetic iron oxide nanoparticles by bacillus cereus strain hmh1: Characterization and in vitro cytotoxicity analysis on mcf-7 and 3t3 cell lines, **270**: 1-11.
.50 Mohapatra, M.;Anand, S.J.I.J.o.E., Science and Technology. (2010). Synthesis and applications of nano-structured iron oxides/hydroxides–a review, **2(8)**.
.51 Mahdy, S.A.;Raheed, Q.J. and

Kalaichelvan, P.J.I.J.o.M.E.R. (2012). Antimicrobial activity of zero-valent iron nanoparticles, **2(1)**: 578-581.

.52 Taylor, E.N.;Kummer, K.M.;Durmus, N.G.;Leuba, K.;Tarquinio, K.M. and Webster, T.J.J.S. (2012). Superparamagnetic iron oxide nanoparticles (spion) for the treatment of antibiotic-resistant biofilms, **8(19)**: 3016-3027.

.53 Arakha, M.;Saleem, M.;Mallick, B.C. and Jha, S.J.S.r. (2015). The effects of interfacial potential on antimicrobial propensity of zno nanoparticle,**5**(110.-1)

.54 Devatha, C.;Thalla, A.K. and Katte, S.Y.J.J.o.c.p. (2016). Green synthesis of iron nanoparticles using different leaf extracts for treatment of domestic waste water, **139**: 1425-1435.

.55 Saranya, S.;Vijayarani, K. and Pavithra, S.J.I.J.o.P.S. .(2017) Green synthesis of iron nanoparticles using aqueous extract of musa ornata flower sheath against pathogenic bacteria, **79(5)**: 688-694.

.56 Basavegowda, N.;Mishra, K. and Lee, Y.R.J.R.A. (2014). Sonochemically synthesized ferromagnetic fe 3 o 4 nanoparticles as a recyclable catalyst for the preparation of pyrrolo [3, 4-c] quinoline-1, 3-dione derivatives, **4(106)**: 61660-61666.

.57 Thomas, J.A.;Schnell, F.;Kaveh-Baghbaderani, Y.;Berensmeier, S. and Schwaminger, S.P.J.C. (2020). Immunomagnetic separation of microorganisms with iron oxide nanoparticles, **8(1)**: 17.

.58 Yi, Y.;Tu, G.;Tsang, P.E.;Xiao, S. and Fang, Z.J.M.L. (2019). Green synthesis of iron-based nanoparticles from extracts of nephrolepis auriculata and applications for cr (vi) removal, 391.-388 :234

.59 Luo, F.;Chen, Z.;Megharaj, M. and Naidu, R.J.R.A. (2014). Biomolecules in grape leaf extract involved in one-step synthesis of iron-based nanoparticles, **4(96)**: 53467-53474.

.60 Katata-Seru, L.;Moremedi, T.;Aremu, O.S. and Bahadur, I.J.J.o.M.L. (2018). Green synthesis of iron nanoparticles using moringa oleifera extracts and their applications: Removal of nitrate from water and antibacterial activity against escherichia coli, **256:** 296-304.

.61 Chandran, S.J.I.J.o.G.P. (2017). Particle size estimation and elemental analysis of yashada bhasma, **11(04)**.

.62 Nguyen, M.D.;Tran, H.-V.;Xu, S. and Lee, T.R.J.A.S. (2021). Fe3o4 nanoparticles: Structures, synthesis, magnetic properties, surface functionalization, and emerging applications, **11**(23.11301